J Mol Model (2013) 19:4089–4097
DOI 10.1007/s00894-012-1717-4

ORIGINAL PAPER

Accuracy of color prediction of anthraquinone dyes in methanol solution estimated from first principle quantum chemistry computations

Piotr Cysewski · Tomasz Jeliński

Received: 1 October 2012 / Accepted: 29 November 2012 / Published online: 19 December 2012

Abstract The electronic spectrum of four different anthraquinones (1,2-dihydroxyanthraquinone, 1-aminoanthraquinone, 2-aminoanthraquinone and 1-amino-2-methylanthraquinone) in methanol solution was measured and used as reference data for theoretical color prediction. The visible part of the spectrum was modeled according to TD-DFT framework with a broad range of DFT functionals. The convoluted theoretical spectra were validated against experimental data by a direct color comparison in terms of CIE XYZ and CIE Lab tristimulus model color. It was found, that the 6-31G** basis set provides the most accurate color prediction and there is no need to extend the basis set since it does not improve the prediction of color. Although different functionals were found to give the most accurate color prediction for different anthraquinones, it is possible to apply the same DFT approach for the whole set of analyzed dyes. Especially three functionals seem to be valuable, namely mPW1LYP, B1LYP and PBE0 due to very similar spectra predictions. The major source of discrepancies between theoretical and experimental spectra comes from L values, representing the lightness, and the a parameter, depicting the position on green→magenta axis. Fortunately, the agreement between computed and observed blue→yellow axis (parameter b) is very precise in the case of studied anthraquinone dyes in methanol solution. Despite discussed shortcomings, color prediction from *first principle* quantum chemistry computations can lead to quite satisfactory results, expressed in terms of color space parameters.

Keywords Anthraquinone · Color · Color computation · TD-DFT · UV–VIS spectrum

Electronic supplementary material The online version of this article (doi:10.1007/s00894-012-1717-4) contains supplementary material, which is available to authorized users.

P. Cysewski (✉) · T. Jeliński
Department of Physical Chemistry, Collegium Medicum, Nicolaus Copernicus University, Kurpińskiego 5, 85-950 Bydgoszcz, Poland
e-mail: piotr.cysewski@cm.umk.pl

T. Jeliński
e-mail: tomasz.jelinski@cm.umk.pl

P. Cysewski
Department of General Chemistry, University of Technology and Life Sciences in Bydgoszcz, Seminaryjna 3, 85-326 Bydgoszcz, Poland

Introduction

Although color determination is of particular importance in many different applications, one has to remember that color perception is a complex human activity involving physical, physiological and psychological counterparts [1]. The color sensation arises from brain activity in response to signals received via the optic nerves from the eyes and this phenomenon is the primary function of photoreceptors built in human eyes [2]. The rods and cones are the two different types of photoreceptors found in the retina of the eye [3] responsible for either a monochromatic light/dark view of the world or color vision [4]. There are three different types of cone cells, labeled as β, γ and ρ, which are sensitive to light of particular wavelength range because of the presence of different opsin types. Short cones (β) absorb light in the wavelength interval of about 400–500 nm (peak maximum at 420–440 nm), medium cones (γ) at about 450–630 nm (maximum at 530–540 nm) and long cones (ρ) at about 500–700 nm (maximum at 560–580 nm) [5]. The resulting color vision comes from the combined effect of stimuli to, and responses from these three different types of cones. The antagonistic and additive response of these types of cone cells corresponds to human color sensation. This assumption was the basis for the formation of so called CIE XYZ color space by the International Commission on Illumination (CIE) in 1931 [6, 7]. Color space is the term for a method for associating tristimulus values with perceived color. Many

mathematical formulations were proposed for quantification of color perception [8] and so called CIE XYZ or CIE Lab standards [9] are the ones of common usage. This three-component standard color space, quantifying three primary contributions to the additive color model, is sufficient to match any perceived color [10]. The distribution of cone cells is not even across the retina and therefore the tristimulus values depend on the observation angle [11]. The so called foveal pit occupies a 2° arc (measured from center of the lens) and since it contains the largest number of cones per unit area it was chosen as the CIE 1931 2° standard observer. The standard observer is characterized by three color matching functions, which represent normalized cone cell response under photopic conditions at medium and high level of illumination. The color-matching functions characterize the amount of XYZ tristimulus (where X = red, Y = green and Z = blue) representing the reflectance or transmittance spectrum weighted by color-matching functions and integrated over the whole spectrum. For actual calculation of tristimulus values XYZ it is necessary to take into account both illuminant spectral power P(λ) and transmittance of transparent media T(λ), (or reflectance in case of opaque materials). Details of mathematical formulations can be found in many available sources dealing with computational color science [8, 9] and will be omitted here.

Anthraquinones are a class of compounds with three fused aromatic rings and two keto groups located on the central ring. The term anthraquinone is usually referred to a specific compound, namely 9,10-anthraquinone (9,10-dioxoanthracene) but many analogues of this compound exist in nature and also many new were synthesized [12, 13]. The fields of application of this class of compounds include medicine [14, 15], dye industry [16] or chemical analysis [17, 18]. Among dihydroxy derivatives of anthraquinones, Alizarin (1,2-dihydroxy-9,10-anthraquinone) (AZ) is probably the most important and the most widely studied dye. Originally, AZ was used as a dye [16] and nowadays it is commonly utilized in medicine, for example in anti-tumor therapy [19, 20], as well as in artwork restoring [21], metal detection [22] and solar energy transformation [23]. Besides the complexation ability of Alizarin has analytical importance [24–26]. Studies have confirmed that Alizarin exists in three different forms, namely the protonated form and two deprotonated forms corresponding to the monoanion and dianion [19, 27, 28]. The spectrum corresponding to the protonated form (in acid solution) is characterized by an absorption maximum of around 430 nm [28–31]. The band with the maximum of around 550 nm corresponds to the monoanionic form, while the dianionic form is represented by two peaks in the range from 570 nm to 620 nm [32, 33]. The 1-amino-2-methylanthraquinone, known also as disperse orange 11 (DO), is a commonly used anthraquinone disperse dye. Such dyes have very low photodecay rates, which is due to their low solubility and therefore their photodegradation process is of particular interest [34]. Dichroism properties of disperse orange 11 have also been studied [35] as well as its usage as image contrast agent [36]. The absorption maximum of this compound is identified by different authors in the region of 470–486 nm [35, 37]. The 1-amino-2-methylanthraquinone exists in two forms, namely the keto and enol forms, the latter of which is less stable [35]. Also a proton transfer from the amino group to the lone oxygen occurs for excited 1-amino-2-methylanthraquinone molecules [34]. Aminoanthraquinones are used traditionally as dyes but their field of application has risen dramatically in the last decades. Thanks to their anticancer activity they have been found to be very useful in medicine [38]. They are also used as electrochromic materials [39]. Their complexes have found applications as sensors [40] or redox-switchable molecules [41]. These wide areas of application have made aminoanthraquinones interesting for academic research. One of the topics of such research is the intra- and inter-molecular hydrogen bonding [42–45] which is thought to have a very significant influence on the properties of amino substituted anthraquinones. The absorption maxima in alcoholic solvent have been identified as 445 nm for 2-aminoanthraquinone [46] and 476 nm for 1-aminoanthraquinone [47].

The time-dependent density functional theory [48] is commonly used for spectra predictions [49]. This is due to its relatively low computational cost when compared to traditional methods. It is achieved because TD-DFT scales the number of molecular orbitals to the fourth power, calculates the frequency dependence of a time-evolution of electrical field and excitation energies as well as transition probabilities their selves are obtained without explicitly calculating the excited states [50]. The effectiveness of TD-DFT and its quite satisfactory agreement with experimental data is recognized in such fields like the description of electronic excitations, response properties, and transport in molecules and in bulk [51, 52]. Among the downsides of this theory one can list the fact that despite its relatively low computational cost it is still too expensive for larger molecular or nano-scaled system, although it is a suitable approach for medium size molecules possessing up to 100 atoms of second row elements [53, 54]. Since there is a wide range of density functionals developed by different authors it is obvious that the choice of the exchange-correlation functional form affects the obtained results. One of the most widely used approximations is the local density approximation (LDA), which depends only upon the value of electronic density at each point in space [55]. One of the approaches among LDA is for example the Perdew-Wang approach [56]. The local density approximation has a tendency of underestimating the values of excitation energies for the majority of organic molecules. Generalized

gradient approximations (GGA) on the other hand, take into account the gradient of the density at the same coordinate and meta-GGA approaches also include the Laplacian of electron density [57]. Functionals of this class include the B98 [58] and M06 [59] ones. These approaches are commonly used for the prediction of UV–VIS spectra. Hybrid functionals, like the Becke3–Lee–Yang–Parr functional (B3LYP) [60], include a component of the exact exchange energy calculated from Hartree–Fock theory.

The aim of this paper is to verify the applicability of TD-DFT approach for description of color of AQs dyes in methanol solution. The accuracy of color prediction is verified against experimental spectra measured in methanol solution. There are many ways of validation of spectra predictions that can be found in the literature. One of the most commonly used approaches is the comparison of band maximum position predicted and measured experimentally. However, there are two shortcomings of this accuracy test. First of all, wave length scale is non-linear and inversely related to transition energy and the inaccuracies in band position do not directly reflect precision, since it is a function of the λ_{max}. Secondly, the practical application of dyes spectra computations should be informative also in terms of commonly used technical parameters. Thus, the color difference seems to be a rational choice, although not commonly applied in the literatures.

Methods

Spectrum measurement of anthraquinones

Methanol of analytical grade purity purchased from POCH (Poland) was used as a solvent. Four anthraquinones, namely 1,2-dihydroxyanthraquinone, 1-amino-2-methylanthraquinone, 1-aminoanthraquinone and 2-aminoanthraquinone come from Sigma Aldrich (USA). Electronic absorption spectra were recorded using single-beam UV/VIS spectrophotometer (Merck, Spectroquant Pharo 300) with wavelength resolution of 1 nm. A solvent blank was measured before each recorded spectrum. All measurements were performed at ambient temperature in standard quartz cuvettes of 1 cm optical length. Six solutions of different concentrations have been measured for each anthraquinone.

Color computation

The main disadvantage of using CIE XYZ color space model [61] is its non-linear nature. Due to this fact, the same changes in tristimulus values for different colors do not correspond to the same alterations of perceived hue. This is why transformations of the XYZ color space were defined. Among many possible formulations [8, 9] the CIE Lab color space [6, 62] is widely used. It defines new parameters, L, a, b, representing psychometric lightness and color change along magenta-green and yellow-blue axes, respectively. The values of lightness (L) can vary from 0, denoting black, up to 100, indicating diffuse white. The negative values of a correspond to green color, while positive represent magenta. The negative values of last parameter, b, represent blue, while positive yellow. Interestingly, these parameters can be used for color difference computations by the following formula:

$$\Delta E = \sqrt{(L^{\exp} - L^{est})^2 + (a^{\exp} - a^{est})^2 + (b^{\exp} - b^{est})^2}, \quad (1)$$

where superscripts *exp* and *est* denote experimental and theoretical values for CIE Lab parameters. When $\Delta E > 5$ it is assumed that the standard observer can see two completely different colors and in the case of $\Delta E > 1$ two colors seem to be indistinguishable.

TD-DFT computations and spectrum deconvolution

Geometries of studied anthraquinones were optimized on B3LYP/6-31G** level with tight criterion for optimization and SCF procedure. The nature of stationary point on the hyperspace was checked by computation of hessian eigenvalues. No imaginary frequencies were noticed, suggesting a correct identification of ground state. This is important due to the fact, that amine side groups can exhibit significant non-planar character and correct improper torsions are mandatory. In both types of computations the ultrafine grid was declared. In this study we have applied a wide range of functionals in order to determine which of them are most suitable for color prediction of the studied group of compounds. Their list can be found in supporting materials (Table S1). Since electronic spectra depend strongly on the solvent used, a proper selection of a solvation model is important. In this paper, PCM with Bondi-type atomic radii parameterization [63, 64] was applied at both geometry optimization and TD-DFT calculation steps. The TD-DFT computations resulted in obtaining the values of electron transition energies and oscillator strengths which were used for convolution of the theoretical spectra. The absorption profiles of UV–VIS spectrum can be decomposed based on a simple additive model of Gaussian-like bands. It is usually satisfactorily accurate for spectroscopic bands with inhomogeneous line broadening as they occur in charge-transfer absorption of large polyatomic molecules in solution. The following formula [65] represents absorption as the function of excitation energy:

$$A(e) = A_o(e) + \sum_{i=1}^{n} 2\sqrt{\ln 2/\pi}\,\frac{f_i}{\sigma_i}\,\exp\left(\frac{-4\ln 2\cdot\left(e_{i,\max} - e\right)^2}{\sigma_i^2}\right), \quad (2)$$

where $A_o(e)$ is the baseline of the spectrum, $e_{i,max}$ is the excitation energy related to wavelength $\lambda_{i,max}$, f_i is the oscillator strength and σ_i is the half-bandwidth of the i-th transition [65]. The deconvolution procedure was performed using Origin 8.0 software [66], which decomposes the spectrum into n-number of formal bands. The single band approximation (SBA) model takes into account only the dominant excitation energy and the number of bands is equal to unity ($n=1$). This approach is appropriate in the case when the optical activity of a compound is limited to one $\pi\rightarrow\pi^*$ excitation. The integrated absorption coefficient (IAC), extracted from the experimental spectrum and defined as $IAC=\int\varepsilon d\nu$, can be computed as the area under optical density (expressed in $dm^3\ mol^{-1}\ cm^{-1}$ units) as a function of the wave number [67, 68] (expressed in cm^{-1}). This leads [69] to the oscillator strength according to the following formula:

$$f = 4.31968 \cdot 10^{-9} \int \varepsilon d\nu. \quad (3)$$

The oscillator strength denotes the number of electrons undergoing particular transition. Typically, its values lies between zero (non allowed transitions) and one (highly intense transitions). The observed properties of optical band responsible for $\pi\rightarrow\pi^*$ excitation were collected in Table 1. This means, that all analyzed dyes exhibit rather modest absorption at the visible part of the spectrum. The values of integrated absorption coefficient are very similar for all analyzed AQs. The Lambert-Beer law is obeyed for all analyzed solutions, although a small associated red-shift, as well as slight peak broadening, can be noticed.

Results and discussion

As has been shown earlier [70] color prediction by means of *first principle* quantum chemistry computations can be quite satisfactory with fairly acceptable agreement with experimental data. We have found, that the most sensitive to model band parameters are red dyes, with absorption bands located in the middle of UV–VIS wavelength range. The prediction of extreme colors, either yellow or blue, is less sensitive to computational inaccuracies. Shifting along red-green axis is generally much more prone to alteration of band parameters than along yellow-blue axis, therefore the changes of the *a* parameter of the CIE Lab model are responsible for the inadequate prediction of λ_{max} in a higher extent than the *b* parameter. This is the reason why color of alizarin in methanol solution is quite accurately predicted by several functional within TD-DFT framework. It is interesting to see if color of other anthraquinones can be computed with comparable accuracy.

Table 1 Experimental values characterizing $\pi\rightarrow\pi^*$ excitation of studied anthraquinone dyes in methanol solutions

	f	λ_{max} [nm]	σ [eV]	$IAC=\int\varepsilon d\nu$ $[dm^3\cdot mol^{-1}\cdot cm^{-1}\ 10^6]$
I	0.107	431.6	0.53	24.7
II	0.091	467.6	0.42	21.4
III	0.084	440.8	0.53	19.5
IV	0.104	468.9	0.43	23.0

DFT functional selection

In Fig. 1 one can find structures analyzed here of AQs, for which UV–VIS spectra were measured in methanol solution with varying concentrations. Based on these data the experimental color was computed according to protocol described in the methodology part. Obtained set of color space parameters constitutes the reference data, against which all theoretical predictions were validated. A series of different functionals, as well as different computational protocols, was applied for prediction of excitation energies of four analyzed anthraquinone dyes. The color was expressed in terms of CIE Lab parameters and was compared to experimental data by the estimation of ΔE values (Eq. 1). The obtained results are provided in Fig. 2 and quantify the color differences between predicted and experimental spectra after averaging over all six concentrations measured for each compound.

In the case of Alizarin, the HSE2PBE functional along with 6-31G** basis set turns out to be the most accurate for color prediction. The color difference between experimental and theoretical CIE Lab values can be as small as 2.5. It is interesting to see that even a modest basis set is satisfactorily accurate for color prediction. Several other functionals, like HSEh1PBE, B972 or B98, perform acceptably well if

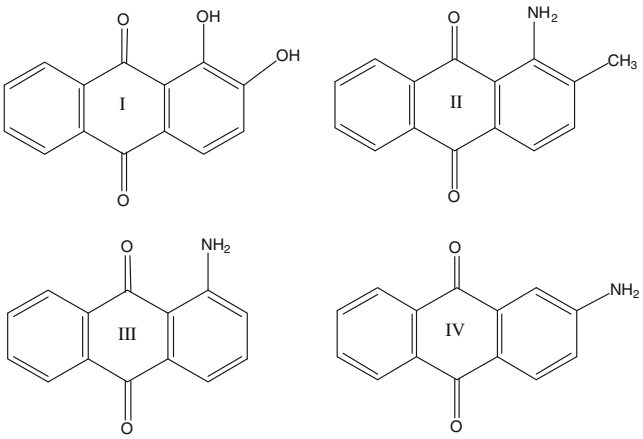

Fig. 1 Molecular formulas of anthraquinone derivatives: 1,2-dihydroxyanthraquinone (I, AZ), 1-amino-2-methylanthraquinone (II, DO), 1-aminoanthraquinone (III) and 2-aminoanthraquinone (IV)

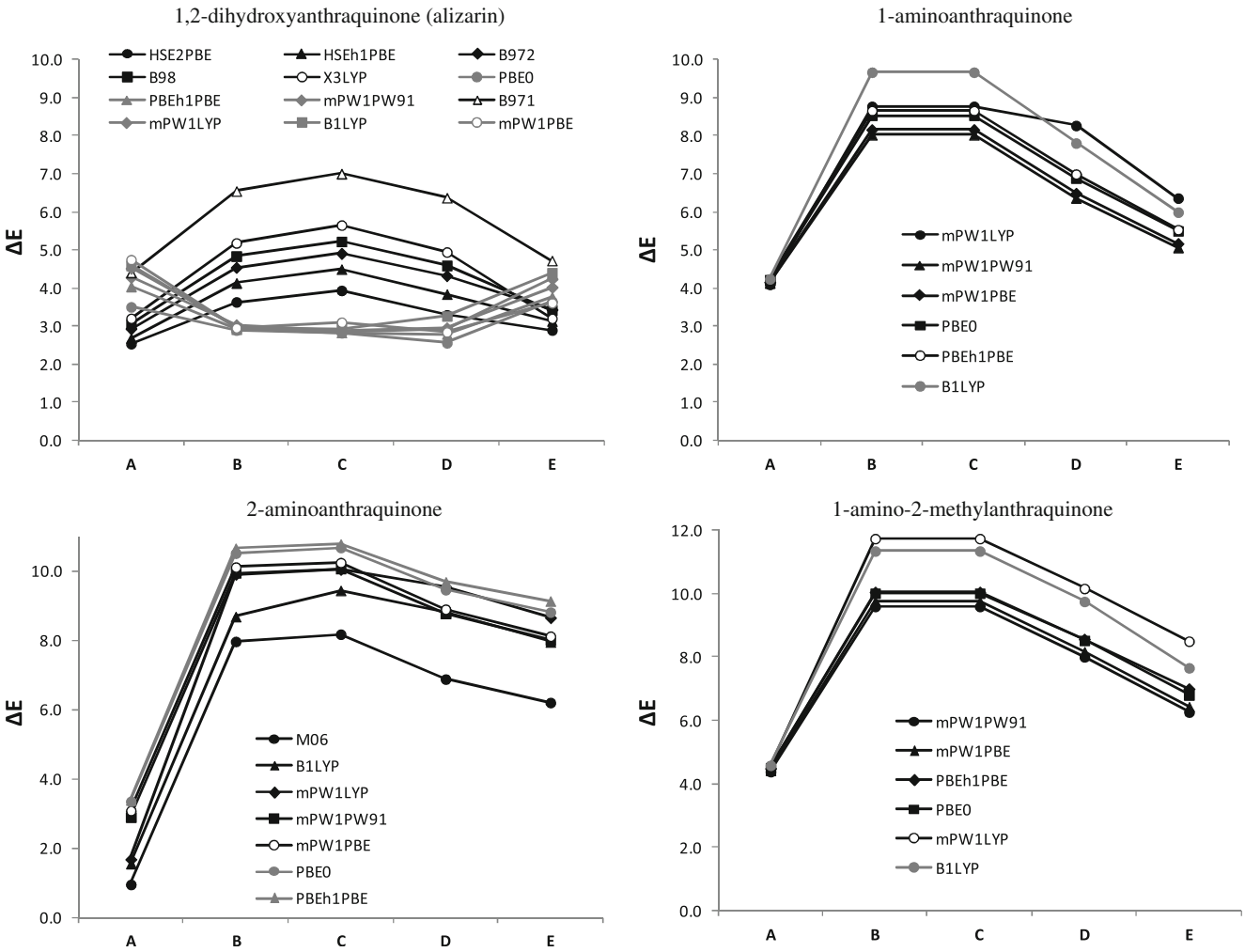

Fig. 2 The accuracy of color prediction by means of a variety of DFT density functionals and computational procedures for anthraquinones in methanol solution. In the following notation, the acronym of basis set used for spectrum estimation precedes the one applied for geometry optimization: A = 6-31G**//6-31G**, B = 6-31++G**//6-31G**, C = 6-311+G**//6-31G**, D = 6-31++G**//6-31++G**, E = 6-311+G**//6-311+G**, F = 6-311++G(2d,2p)//6-311++G(2d,2p)

6-31G** basis set is used. Interestingly, the most commonly applied functional for spectra prediction, PBE0, leads to slightly worse color description of AZ in methanol solution. Another interesting observation is the fact, that for AZ two classes of functionals can be found, the accuracy of which depends on the level of the basis set used. The first class comprises those functionals for which the extension of the basis set decreases the accuracy in color prediction and only using the richest 6-311++G (2d,2p) allows for a comparable ΔE value. Other procedures, like B–E, lead to significantly less accurate color prediction. For the functionals of the second class those procedures perform best, while the procedures A and F are less accurate. This can be attributed to the red-shift of predicted λ_{max} with respect to experimental ones. Thus, extension of the basis sets is only sensible for such functionals, which underestimate λ_{max} value, for there is a chance that resulting red-shift reduces the $\Delta\lambda_{max}$ error. This dual behavior of DFT functionals is not observed here for other studied anthraquinone dyes. To the contrary, for all amino-substituted anthraquinones the extension of the basis reduces accuracy of color prediction. This is related to the fact that for these dyes all functionals underestimate the position of the only band in visible region. In the case of 1-aminoanthraquinone, the lowest values of ΔE were obtained using hybrid functional of Truhlar and Zhao, M06 funcional [59]. The color of other two AQs is described with highest accuracy with an aid of parameter hybrid functional using modified [71] Perdew-Wang exchange combined with either PW91 or LYP correlations. The situation described above is slightly discouraging since no single DFT protocol emerges from above analysis. However, future investigation of other dyes cannot be performed using different functionals for different compounds. Thus, a close inspection into the balanced solutions for all studied dyes seem to be indispensible.

Table 2 The values of color difference (ΔE) between experimental and theoretical color estimated for studied anthraquinones by means of different functionals and computations on level A (6-31G**//6-31G**)

DFT functional	I	II	III	IV	Mean
mPW1LYP	4.52	1.68	4.10	4.57	3.72
B1LYP	4.59	1.55	4.24	4.59	3.74
PBE0	3.51	3.35	4.22	4.50	3.90
mPW1PW91	4.28	2.90	4.13	4.38	3.92
PBEh1PBE	4.04	3.39	4.24	4.50	4.04
mPW1PBE	4.75	3.08	4.16	4.43	4.10
M06	5.76	0.95	5.59	5.63	4.48
HSEh1PBE	2.69	9.75	8.90	10.06	7.85

In Table 2 the mean values of error in color prediction were collected. Although color of each compound can be described by different method, the cumulative values for the set of all four anthraquinone dyes do not differ significantly between several functionals and most of them are able to predict color with threshold accuracy of $\Delta E<5.0$. The mean values are within half of an energy change unit for all functionals mentioned in Table 2, except the last one, HSEh1PBE. Thus, all these might be of potential use. It is worth mentioning, that ΔE is very sensitive to even minute changes in the spectrum. This is clearly visible in Fig. 3 comprising spectra predicted with the use of three most appropriate functionals described in Table 2. The correlation between the predicted and experimental spectra is very good for all the compounds, which emphasizes the conclusion that the application of TD-DFT methods can lead to quite acceptable color prediction.

Sensitivity of λ_{max} to amount of HF exchange contribution

Hybrid functionals are a class of approximations to the exchange-correlation energy functional, incorporating mixtures of some fraction of exact exchange from Hartree-Fock (HF) theory with exchange and correlation from other sources. Although the actual amount of gradient correction to the exchange and the correlation contributions can be set independently, many popular hybrid functionals have fixed values. In the case of PBE functional, exchange and gradient-corrected correlation functionals were introduced by Perdew, Burke and Ernzerhof [72, 73]. As was nowadays demonstrated in the paper by Kantchev et al. [74] the percentage of HF exchange in the hybrid GGA DFT approaches can be quite an important factor limiting the accuracy of λ_{max} predictions. For example, hybrid functional PBE0 (known also as PBE1PBE) uses a 1 to 3 mixture of DFT and exact exchange energies: $E_{XC} = 0.25 \cdot E_X(HF) + 0.75 \cdot E_X(PBE) + E_C(mPW91)$. Thus, PBE0 has only one parameter, which can be adjusted. It is interesting how sensitive the predictions are

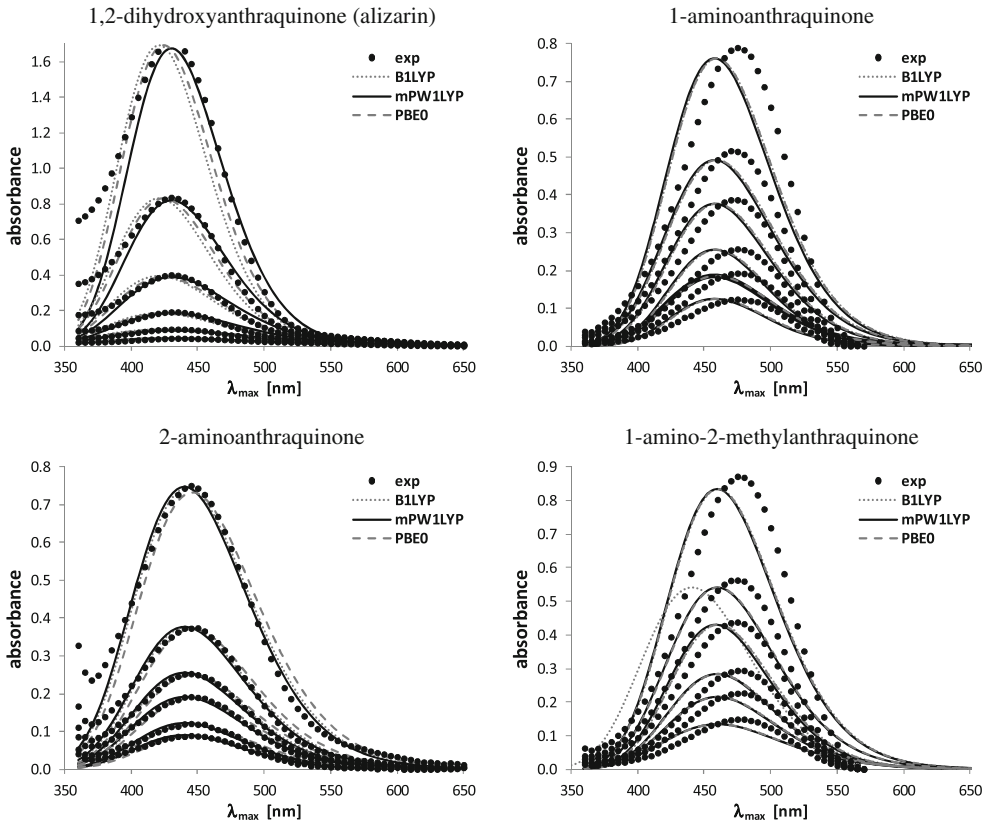

Fig. 3 The predicted spectra of anthraquinones imposed on experimental ones for studied anthraquinone dyes in methanol solution

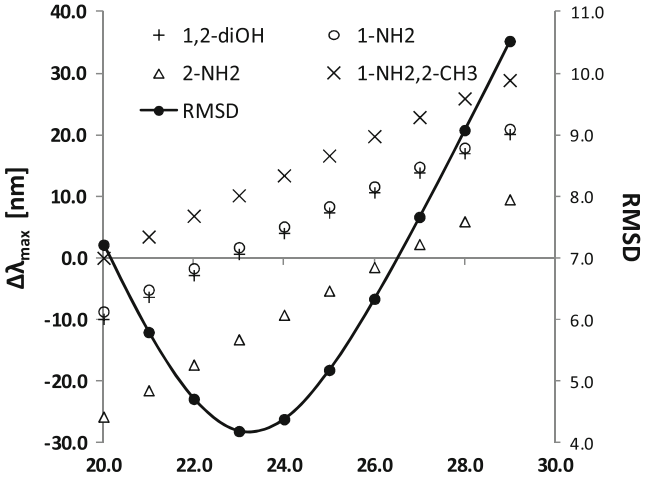

Fig. 4 The influence of the percentage of HF exchange in PBE0 functional on $\Delta\lambda_{max} = \lambda_{max,exp}-\lambda_{max,est}$ (expressed in nm). The minimum on RMSD curve corresponds to 23.2 %

of λ_{max} for studied here anthraquinone dyes on the percentage of HF exchange. Results of a systematic study are presented in Fig. 4. Indeed, the provided data suggest a very high sensitivity of optical properties of AQs on E_X(HF) percentage. Small changes, even within a few percent, lead to a dramatic deviation of computed band position with respect to the observed ones. The relationship is almost linear and for all four studied AQs the higher HF exchange contribution the stronger underestimation of λ_{max}. The optimal value of adjusted parameter is somewhat different for particular anthaquinone dyes. Based on cumulative RMSD the best value of E_X(HF) contribution was found to be equal to 23.2 % in the case of PBE0 functional. Since this value is not far from the default one (25 %), it seems that the application of this adjustment to a broad range of anthaquinone dyes is not justified since it is case-dependent.

Color prediction

The agreement between the CIE Lab color parameters for the experimentally obtained and computed spectra is presented in Fig. 5. It is clearly visible, that with the increase of anthraquinone concentration the difference between the experimental and theoretical values of the L (lightness) parameter increases. This trend is also observed for the parameter a, which corresponds to color change along the green→magenta axis. However, these differences are not identical among all of the studied anthraquinones. For example, when considering this parameter, the difference for alizarin is quite small, while for other anthraquinones it is significantly larger and is the largest in the case of 2-aminoanthraquinone. The agreement between the experimental and theoretical values is much better in the case of b parameter and observed differences are comparable for all anthraquinones.

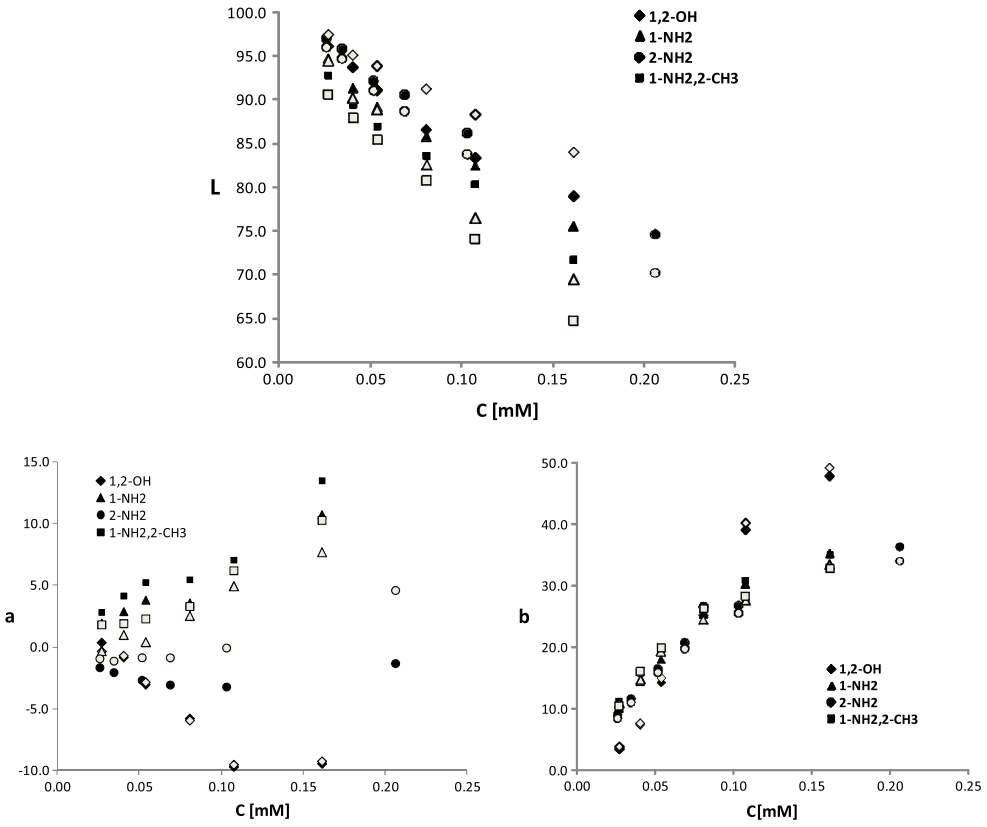

Fig. 5 The comparison of experimental and theoretical values of CIE Lab parameters. Black symbols represent values obtained based on observed spectra, while open symbols stand for data computed using PBE0/6-31G**//6-31G** level

Conclusions

The single band approximation (SBA) model gives satisfactory color prediction in the framework of CIE XYZ or CIE Lab standards. The assumption of a Gaussian-like shape of the band is quite accuracy in color prediction from TD-DFT calculations. The accuracy of such prediction depends on both the basis set used and the applied functional. The relatively modest 6-31G** basis set is sufficiently accurate for color prediction in the case of all anthraquinones studied here. This is not a new observation and confirms previous observation made in the sense of λ_{max} predictions [28, 53]. The extension of the basis set does not improve the accuracy of color estimation and although in the case of Alizarin the richest basis set also provides quite satisfactory results the cost of computations makes this rather uneconomic. A variety of functionals leads to quite accurate color estimation with $\Delta E<5$. The HSE2PBE functional is most accurate in the case of Alizarin, mPW1PW9 functional gives the best prediction for 1-amino-2-methylanthraquinone while the mPW1Lyp and M06 functionals perform best in the case of 1-aminoanthraquinone and 2-aminoanthraquinone, respectively. When taking into account the mean value of ΔE calculated for the four compounds it can be concluded that several functionals can be universally used for color prediction since their mean value of color difference is on a satisfactory level. Among them, the mPW1LYP, B1LYP and PBE0 functionals give the best mean accuracy. The obtained results confirm our earlier observation that the color prediction from *first principle* quantum chemistry computations can lead to quite satisfactory results expressed in terms of color space parameters. The presented bridge linking quantum chemistry spectra predictions with technical parameters can be widely applied for new material design. On the other hand, the knowledge of limitations and accuracy of current state theory discussed in the paper is worthy itself in the context of future applications. Among these restrictions, it is worth emphasizing again that the higher dye concentrations the discrepancy in predicted and estimated lightness (L parameter) is more pronounced. Also, a similar trend is observed for green→magenta axis (parameter a). Fortunately, the agreement between computed and observed blue→yellow axis (parameter b) is quite acceptable in the case of studied anthraquinone dyes in methanol solution.

Acknowledgments Results were obtained as the part of computational grant no 104 of Poznań Supercomputing and Networking Center (Poznań, Poland) and Academic Computer Centre CYFRONET within PlGrid infrastructure. The allocation of computational facilities is greatly appreciated.

References

1. Graham CH (1965) Vision and visual perception. Wiley, New York
2. Hurvich LM, Jameson D (1957) Psychol Rev 64:384–404
3. Zollinger H (2001) Color chemistry. Wiley, New York
4. Curcio J, Sloan CAKR et al. (1990) J Comp Neurol 292:497–523
5. Wyszecki G, Stiles WS (1982) Color science: concepts and methods. Quantitative data and formulae. Wiley, New York
6. CIE. Commission Internationale de l'Eclairage (1932) Proceedings, 1931. Cambridge University Press, Cambridge
7. Smith T, Guild J (1931) Trans Opt Soc 33:73–34
8. Westland S, Ripamonti C (2004) Computational colour science, using MATLAB. Wiley, Chichester
9. Schanda J (2007) Colorimetry. Understanding the CIE system. Wiley, New York
10. Hunt RW (1998) Measuring colour. Fountain Press, Tolworth, UK
11. Harrison ER (1953) Br J Ophthalmol 37:538–542
12. Singh R, Geetanjali J (2005) Serb Chem Soc 70:937–942
13. Madje BR, Shelke KF, Sapkal SB, Kakadze GK, Shingare MS (2010) Green Chem Lett Rev 3:269–273
14. Bányai P, Kuzovkina N, Kursinszki L, Sz ke É (2006) Chromatogr Suppl 63:111–114
15. Huang Q, Lu G, Shen HM, Chung MCM, Ong CN (2007) Interscience 27:609–630
16. Angelini LG, Pistelli L, Belloni P, Bertoli A, Panconesi S (1997) Indust Crops Products 6:303–311
17. Canamares MV, Ramos JVG, Domingo C, Cortes SS (2004) J Raman Spectrosc 35:921–927
18. Mascaros SM, Domingo C, Cortes SS, Canamares MV, Ramos JVG (2005) J Raman Spectrosc 36:420–426
19. Das S, Bhattacharya A, Mandal PC, Rath MC, Mukherjee T (2002) Radiat Phys Chem 65:93–100
20. Berman HM, Young PR (1981) Annu Rev Biophys Bioengng 10:87–114
21. Murcia-Mascarós S, Domingo C, Sanchez-Cortes S, Cañamares MV, Garcia-Ramos JV (2005) J Raman Spectrosc 36:420–426
22. Fain VY, Zaitsev BE, Ryabov MA (2004) Russ J Coord Chem 30:365–370
23. Sánchez-de-Armas R, Oviedo López J, San-Miguel MA, Sanz JF, Ordejón P, Pruneda M (2010) J Chem Theory Comput 6:2856–2865
24. Ge F, Jiang L, Liu D, Chen C (2011) Anal Sci 27:79–84
25. Downard A, Powell H, Kipton J, Xu S (1991) Anal Chim Acta 251:157–163
26. Khalifa ME (1996) Chem Anal 41:357–362
27. Fain VY, Zaitsev BE, Ryabov MA (2004) Russ J Gen Chem 74:1558–1563
28. Preat J, Laurent A, Michaux C, Perpete E, Jacquemin D (2009) J Mol Struct 901:24–30
29. Milliani C, Romani A, Favaro G (2000) J Phys Org Chem 13:141–150
30. Sasirekha V, Umadevi M, Ramakrishnan V (2008) Spectrochim Acta A 69:148–155
31. Say-Liang-Fat S, Cornard JP (2011) Polyhedron 30:2326–2332
32. Quinti L, Allen N, Edge M, Murphy B, Perotti A (2003) J Photochem Photobiol A 155:93–106
33. Savko M, Kasackova S, Gbur P, Miskovsky P, Ulicny J (2007) J Mol Struct 823:78–86
34. Chu W, Tsui SM (2001) J Environ Eng 127:741–747
35. Abbas B, Alshikh Khalil M (2010) Acta Phys Pol A 117:904–910
36. Jones GB, Xie L, El-Shafey A et al. (2004) Bioorg Med Chem Lett 14:3081–3084
37. Joung SM, Yoo KP (1998) J Chem Eng Data 43:9–12
38. Butler J, Hoey BM (1987) Br J Cancer Suppl 8:53–59
39. Gater VK, Lui MD, Love MD, Leidner CR (1988) J Electroanal Chem 257:133–146
40. Wasielewski MR (1992) Chem Rev 92:435–461
41. Echegoyen LE, Yoo HK, Gatto VJ, Gokel GW, Echegoyen L (1989) J Am Chem Soc 111:2440–2243

42. Dahiya P, Kumbhakar M, Mukherjee T, Pal H (2006) J Mol Struct 798:40–48
43. Dahiya P, Kumbhakar M, Maity DK et al. (2006) J Photochem Photobiol A 181:338–347
44. Müller C, Schroeder J, Troe J (2006) J Phys Chem B 110:19820–19832
45. Ponomareva RP, Studzinskii OP, Borisova LM (2002) Russ J Gen Chem 72:1104–1106
46. Dibrova VM, Nurmukhametov RN, Klimenko VG, Vostrova VN (1991) J Appl Scpect 55:1001–1006
47. Klimenko VG, Yakovlev Y, Nurmukhametov RN (1989) J Appl Scpect 50:575–578
48. Runge E, Gross EKU (1984) Phys Rev Lett 52:997–1000
49. Fleming S, Mills A, Tuttle T, Beilstein J (2011) Org Chem 7:432–441
50. Van Gisbergen SJA, Guerra CF, Baerends EJ (2000) J Comput Chem 21:1511–1523
51. Casida ME (1995) Recent advances in density functional methods. World Scientific, Singapore
52. Marques CA, Ullrich MAL, Nogueira F, Rubio A, Burke K, Gross EKU (2006) Time-dependent density functional theory. Springer, Heidelberg
53. Jacquemin D, Perpète EA, Ciofini I, Adamo C (2009) Acc Chem Res 42:326–334
54. Fabian J (2010) Dyes Pigm 84:36–50
55. Parr RG, Yang W (1994) Density-functional theory of atoms and molecules. Oxford University Press, Oxford
56. Perdew JP, Wang Y (1992) Phys Rev B 45:13244–13249
57. Cramer CJ (2004) Essentials of computational chemistry. Wiley, New York
58. Schmider HL, Becke AD (1998) J Chem Phys 108:9624–9631
59. Zhao Y, Truhlar DG (2008) Theor Chem Acc 120:215–241
60. Becke AD (1993) J Chem Phys 98:5648–5652
61. Broadbent AD (2004) Color Res Appl 29:267–272
62. Netravali AN, Haskell BG (1986) Digital pictures: representation, compression, and standards. Springer, Heidelberg
63. Miertuš S, Scrocco E, Tomasi J (1981) Chem Phys 55:117–129
64. Miertuš S, Tomasi J (1982) Chem Phys 65:239–245
65. Hollas JM (1982) High resolution spectroscopy. Butternorth
66. OriginLab (2007) Origin ver. 8.0. OriginLab, Northampton
67. Sturm JE (1990) J Chem Educ 67:32–33
68. Sturm JE (1992) J Chem Educ 69:686–688
69. Barrow GM (1962) Introduction to molecular spectroscopy. McGraw-Hill, New York
70. Cysewski P, Jelinski T, Przybyłek M, Shyichuk A (2012) New J Chem 36:1836–1843
71. Adamo C, Barone V (1998) J Chem Phys 108:664–675
72. Perdew JP, Burke K, Ernzerhof M (1996) Phys Rev Lett 77:3865–3868
73. Perdew JP, Burke K, Ernzerhof M (1997) Phys Rev Lett 78:1396–1396
74. Kantchev EAB, Norsten TB, Sullivan MB (2012) Org Biomol Chem 10:6682–6692